International Journal of Heat and Mass Transfer 52 (2009) 2026–2041

Contents lists available at ScienceDirect

International Journal of Heat and Mass Transfer

journal homepage: www.elsevier.com/locate/ijhmt

Analysis of the vaporization process for a nano-scale liquid thread by molecular dynamics simulation

Chun-Lang Yeh *

Department of Aeronautical Engineering, National Formosa University, No. 64 Wen-Hua Rd., Huwei, Yunlin 632, Taiwan, ROC

ARTICLE INFO

Article history:
Received 13 March 2008
Received in revised form 20 October 2008
Available online 26 December 2008

Keywords:
Nano-scale liquid thread
Vaporization process
Molecular dynamics simulation

ABSTRACT

The vaporization process of a nano-scale liquid thread in vapor or vacuum is analyzed by molecular dynamics simulation. The formation of liquid threads is one of the most fundamental and important phenomena during the atomization process. The analyses in the existing literatures for this topic were performed only down to the stage of formation of liquid particles. The present analysis focuses not only on the liquid particle formation but also on its subsequent evolution, which plays an important role in the entire vaporization process. In this study, snapshots of the molecules, evolution of the density field, and evolution of the intermolecular force are analyzed. Finally, the Rayleigh's stability criterion is assessed for its validity in molecular scale.

1. Introduction

Investigation of the atomizer flow receives considerable attentions because of its wide range of applications in many fields, e.g. industrial processes, agriculture, meteorology, medicine, etc. A conventional way for the atomizer flow research is to conduct experimental investigations of large-scale models. Historically, less attention has been devoted to the internal flow development in atomizers due to the small size of practical atomizers, which makes measurements difficult. Another approach for the atomizer flow research is to do detailed numerical simulations. An advantage of the numerical simulations is that practical-scale atomizers can be studied as easily as large scale ones. A comprehensive literature review for the experimental and numerical investigations of the atomizer flow has been done in the author's previous studies [1–6]. Numerical simulation of the atomizer flow can be roughly divided into two categories, namely, the macroscopic analysis and the microscopic analysis, each with its own advantages and disadvantages. The former one is principally based on the computation of the Navier–Stokes equations and is usually adopted for the purpose of atomizer parametric study due to its relatively lower computational cost. In the author's previous studies [1–6], a series of analyses for the atomizer internal and external flows have been conducted. The macroscopic behavior and characteristics of the atomizer flow, such as discharge coefficient, spray angle, film thickness, atomizer geometry, etc. were analyzed. However, when liquid breaks up into ultra-fine nano-scale droplets, the Navier–Stokes equations, which are derived based on continuum concept, are no longer valid for simulation of the subsequent atomization process. The author's previous studies were therefore confined to the investigation of the earlier stage of atomization process, during which the breakup phenomenon had not yet happened. In order to overcome this inherent deficiency, the macroscopic analysis has to be replaced by the microscopic analysis for later stage of the atomization process.

In Fig. 1, the fluid/air interface for atomizer flow by the macroscopic analysis from one of the author's previous studies [3] is shown. It can be seen that the liquid evolves into threads after leaving the atomizer. The formation of liquid threads is one of the most fundamental and important phenomena during the atomization process. Koplik and Banavar [7] studied the Rayleigh instability of a cylindrical liquid thread in vacuum by three-dimensional molecular dynamics (MD) simulation. The maximum number of molecules they used consists of 8192 liquid argon Lennard–Jones molecules for a cylindrical liquid thread of non-dimensionalized radius of 7.5 in a box of non-dimensionalized length of 54.7. For this simulation condition, only one liquid particle was formed. If a smaller computational domain was used instead, no liquid particle was found from their study. Kawano [8] applied 10278 Lennard–Jones molecules of liquid and vapor coexisting argon in three dimensions to analyze the interfacial motion of a cylindrical liquid thread of non-dimensionalized radii of 2.0–4.0 in a box of maximum non-dimensionalized length of 120. For this condition of larger computational domain, a maximum number of 8–9 liquid particles were observed. Min and Wong [9] studied the Rayleigh instability of nanometer scale Lennard–Jones liquid threads by MD simulation and found that Rayleigh's continuum prediction holds down to the molecular scale. Kim et al. [10] applied MD simulation to investigate the thermodynamic properties and stability

* Tel.: +886 5 6315527; fax: +886 5 6312415.
E-mail address: clyeh@nfu.edu.tw

0017-9310/$ - see front matter © 2008 Elsevier Ltd. All rights reserved.
doi:10.1016/j.ijheatmasstransfer.2008.10.026

Nomenclature

F	intermolecular force
k_B	Boltzmann constant
L	fundamental cell characteristic length
m	molecular mass
N	number of molecules
R	liquid thread radius
r	intermolecular distance
r_c	cut-off radius of Lennard–Jones potential function
T	temperature
t	time
Δt	time step
V	volume
v_i	velocity of molecule i
x,y,z	Cartesian coordinates

Greeks

ε	energy parameter of Lennard–Jones potential function
ρ	density
σ	length parameter of Lennard–Jones potential function
φ	Lennard–Jones potential function

Subscripts

L	liquid phase
V	vapor phase

Superscripts

*	non-dimensionalized quantity
–	averaged quantity

characteristics of the nano-scale liquid thread. Density and pressure profiles, as well as properties such as equimolar dividing radius, radius of surface tension, and surface tension were determined in their study.

In the above MD studies of liquid threads [7–10], the analyses were performed only down to the stage of the formation of liquid particles. Subsequent evolution, which involves breakup, collision, and coalescence of the liquid particles, were not analyzed in detail. However, these phenomena play important roles in the entire vaporization process. The present analysis therefore focuses not only on the liquid particle formation but also on its subsequent evolution, with the aim to provide a detailed illustration for the vaporization process of a liquid thread.

2. Molecular dynamics simulation method

In this study, the vaporization process of a liquid thread is investigated by MD simulation. The inter-atomic potential is one of the most important parts of MD simulation. Many possible potential models exist, such as hard sphere, soft sphere, square well, etc. [11]. In this research, the Lennard–Jones 12-6 potential model, which is widely used, is adopted for calculation. It is

$$\phi(r) = 4\varepsilon\left[\left(\frac{\sigma}{r}\right)^{12} - \left(\frac{\sigma}{r}\right)^{6}\right] \tag{1}$$

where r denotes the distance between two molecules, ε and σ are the representative scales of energy and length, respectively. The Lennard–Jones fluid in this research is taken to be argon for its ease of physical understanding. The parameters for argon are as follows [8]: the length parameter $\sigma = 0.354$ nm, the energy parameter $\varepsilon/k_B = 93.3$ K, and the molecular weight $m = 6.64 \times 10^{-26}$ kg, where $k_B = 1.38 \times 10^{-23}$ J/K denotes the Boltzmann constant. The cut-off radius r_c beyond which the intermolecular interaction is neglected is 5.0σ.

The simulation domain is schematically shown in Fig. 2, with periodic boundary conditions applied in all three directions. Simulation domain dimensions, number of molecules and number densities are listed in Table 1, together with some simulation results. The time integration of motion is performed by Gear's fifth predictor–corrector method [11] with a time step of $\triangle t^* = 0.001$(i.e. 2.5 fs). Note that all quantities with an asterisk in this paper, such as L^*, R^*, ρ^*, $\triangle t^*$, etc., are non-dimensionalized in terms of σ, ε, and m, i.e. $L^* = L/\sigma$, $R^* = R/\sigma$, $\rho^* = N\sigma^3/V$, $\triangle t^* = \triangle t\,(\varepsilon/m)^{1/2}/\sigma$, $T^* = k_B T/\varepsilon$.

In this research, a cylindrical liquid thread of length L^* and radius R^* is placed at the center of the computational domain and the remaining space is either in vacuum or filled with vapor

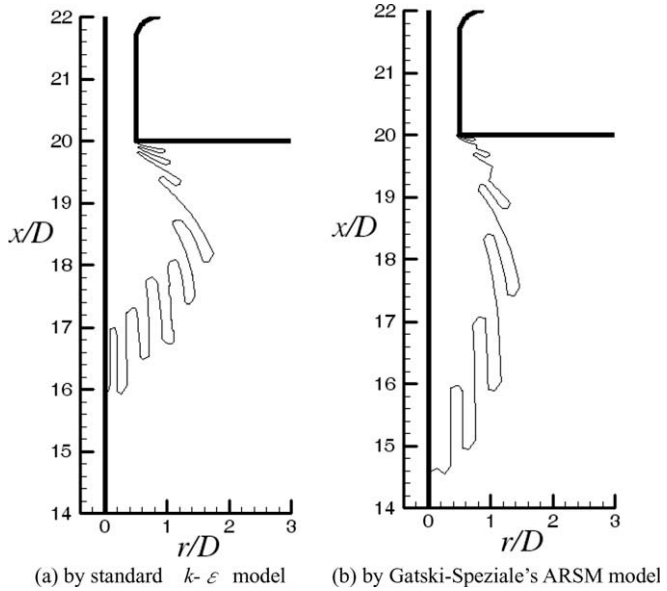

Fig. 1. Fluid/air interface for atomizer flow by macroscopic analysis [3].

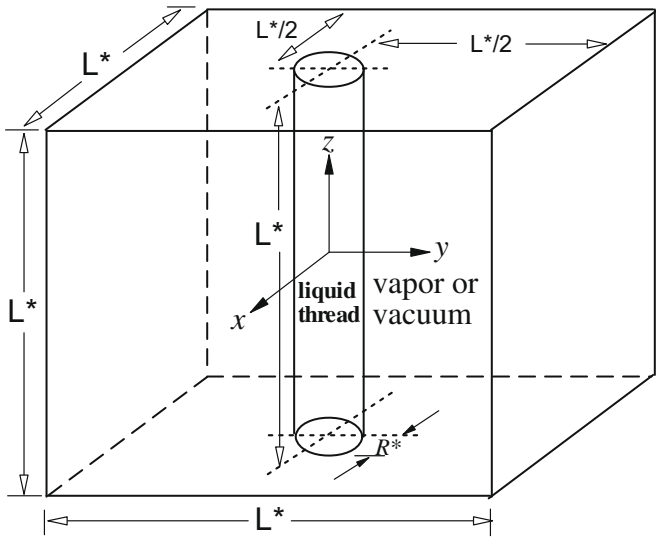

Fig. 2. Illustration of the computational domain for the simulation of a liquid thread.

Table 1
Simulation domain dimensions, number of molecules, number densities, and simulation results (L^* = 120, $\rho_L^* = 0.819$).

Case No.	R^*	N_{mol}	ρ_V^*	$\overline{f_\rho}$	$\overline{F}^*$
1	2	6559	0.0031	0.291	1.458
2	3	8090	0.0031	0.309	2.592
3	4	10,254	0.0031	0.332	3.801
4	5	12,965	0.0031	0.362	5.051
5	2	1225	Vacuum	0.325	6.874
6	3	2762	Vacuum	0.494	10.716
7	4	4934	Vacuum	0.478	10.631
8	5	7651	Vacuum	0.656	14.267

molecules. The initial densities of the liquid and vapor are $\rho_L^* = 0.819$ and $\rho_V^* = 0.0031$ or 0, respectively. The system temperature is kept at $T^* = 0.75$. These dimensionless values correspond to $\rho_L = 1223\ kg/m^3$, $\rho_V = 4.63\ kg/m^3$ or 0 for argon and $T = 70\ K$. The computational conditions of ρ_L^*, ρ_V^* and T^* are chosen considering the phase diagram of the Lennard–Jones fluids [8], that is, the values of ρ_L^*, and ρ_V^* are set to be the liquid and vapor densities, respectively, in the coexistence properties for the Lennard–Jones fluids and T^* is kept at a value above the triple point temperature throughout the vaporization process.

The procedure for MD simulation includes three stages: initialization, equilibration and production. Because the simulation domain comprises a cylindrical liquid thread and its surroundings (either vapor or vacuum), it is difficult to retain the density and cylindrical geometry of the liquid thread if the equilibration stage is performed under the condition of liquid thread coexisting with vapor. Therefore, the vapor and liquid molecules are equilibrated individually. Initially, equilibration is performed for liquid mole-

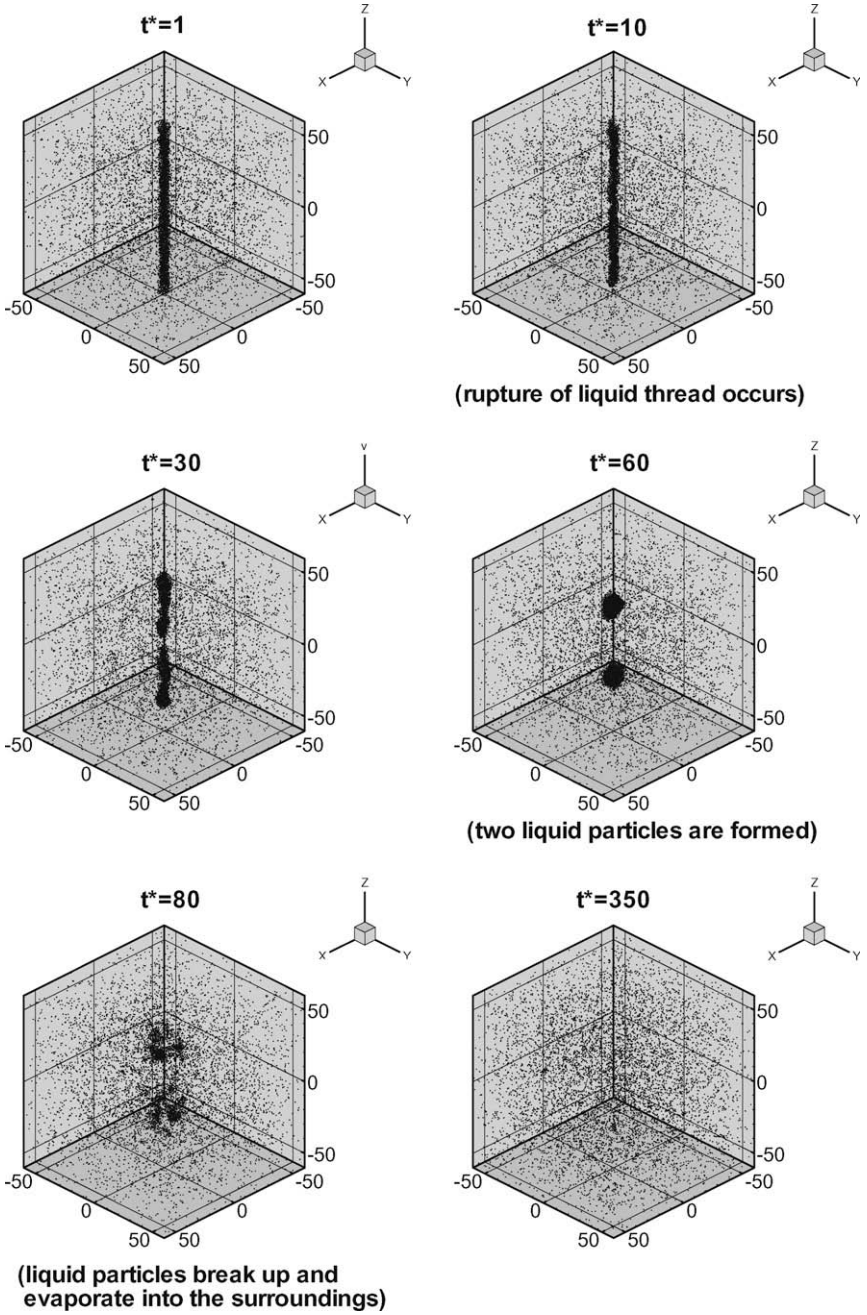

Fig. 3. Vaporization process for case 2 in Table 1.

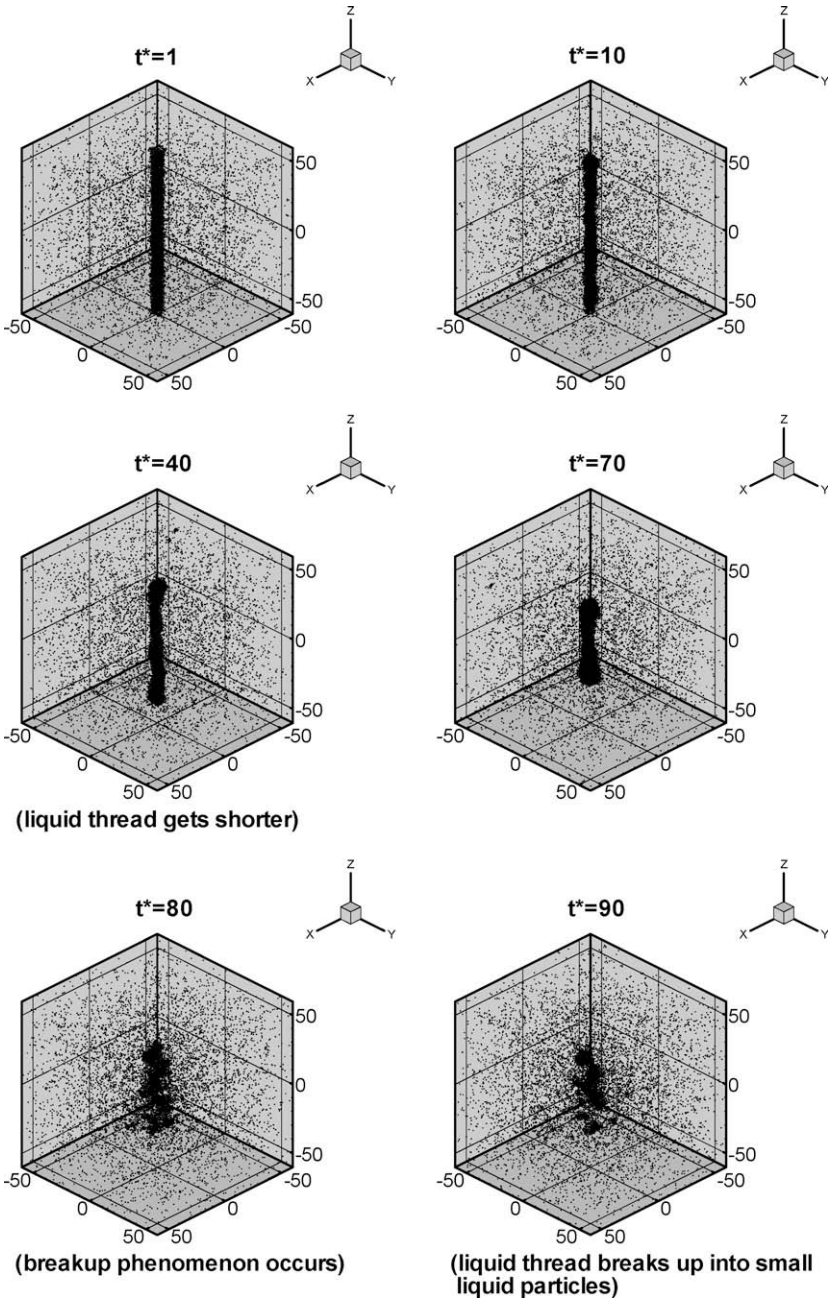

Fig. 4. Vaporization process for case 3 in Table 1.

cules in a rectangular parallelepiped with length and width equal to the liquid thread diameter ($D^* = 2R^* = 4$, 6, 8 or 10) and with height equal to the side length of the computational domain ($L^* = 120$). The initial velocities of molecules are decided by the use of normal random numbers. Velocity rescaling is performed at each time step by Eq. (2) to make sure that the molecules are at the desired temperature T^*:

$$v_i^{new} = v_i^{old}\sqrt{\frac{T_D}{T_A}} \tag{2}$$

where v_i^{new} and v_i^{old} are the velocities of molecule i after and before correction, respectively, and T_D and T_A are the desired and the actual molecular temperatures, respectively. Similarly, equilibration is performed for vapor molecules in a cube of congruous geometry to the simulation domain (a cube of side length $L^* = 120$). The vapor and liquid molecules are equilibrated individually for 10^6 time steps at the desired temperature T^*. The achievement of the equilibrium state is confirmed by obtaining the radial distribution function. After the liquid and vapor molecules are equilibrated, the rectangular parallelepiped for the liquid molecules and the cube for the vapor molecules are truncated to the desired cylindrical liquid thread and surrounding vapor, respectively, by removing unwanted regions. Then the cylindrical liquid thread and the surrounding vapor are put together into the computational domain and the production stage proceeds. A minimum image method and the Verlet neighbor list scheme [11] to keep track of which molecules are actually interacting at a given time interval of 0.005 are used in the equilibration and production stages.

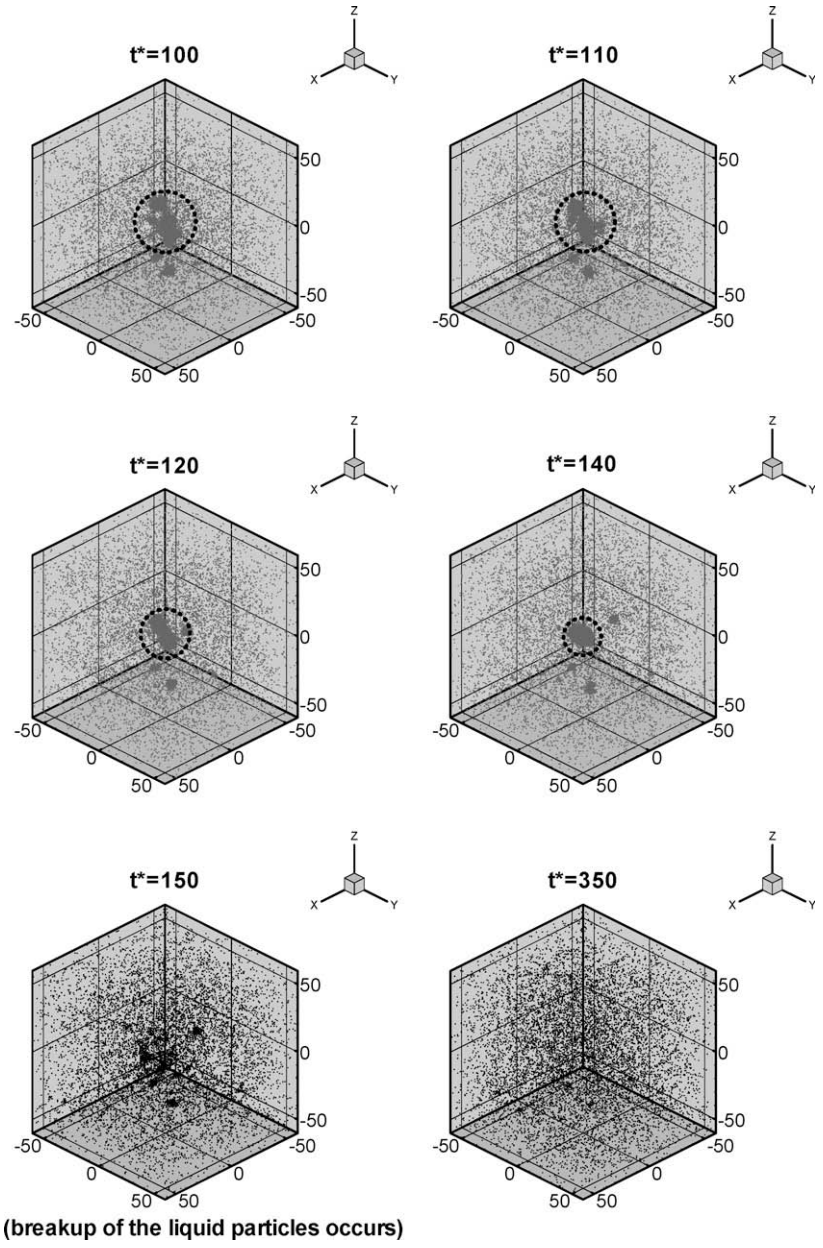

Fig. 4 (*continued*)

3. Results and discussions

3.1. Liquid thread vaporization process

In the following discussion, a cylindrical liquid thread of length L^* and radius R^* is placed at the center of the simulation domain and the remaining space is either in vacuum or filled with vapor molecules, as illustrated in Fig. 2. Simulation domain dimensions, number of molecules and number densities are listed in Table 1.

3.1.1. Liquid thread in vapor

Fig. 3 shows the vaporization process of a liquid thread of $L^* = 120$ and $R^* = 3$, which corresponds to $L = 42.5$ nm and $R = 1.06$ nm. The dot in Fig. 3 indicates the center of the molecule. It is found that rupture of the liquid thread occurs at about $t^* = 10$ both from its middle section and from its two ends, i.e. the top and bottom surfaces of the fundamental cell. After $t^* = 10$, the molecules evolve into liquid particles by the contraction motion of molecules in the axial direction of the liquid thread. Two liquid particles are formed at about $t^* = 60$ and they break up and evaporate into the surroundings at about $t^* = 80$. If the radius of the liquid thread becomes larger, say $R^* = 4$, no rupture of the liquid thread in the interior of the fundamental cell is found, as can be observed from Fig. 4. The liquid thread ruptures only from its two ends, i.e. the top and bottom surfaces of the fundamental cell, and gets shorter due to the contraction motion in its axial direction. Breakup phenomenon occurs at about $t^* = 80$. The liquid thread disintegrates into small liquid particles first ($t^* = 90$) and then evaporates into the surroundings. During the subsequent vaporization process ($t^* \geqq 100$), it is observed that collision, coalescence, and breakup of the liquid particles occurs. Collision and coalescence of the liquid particles can be seen in the portions

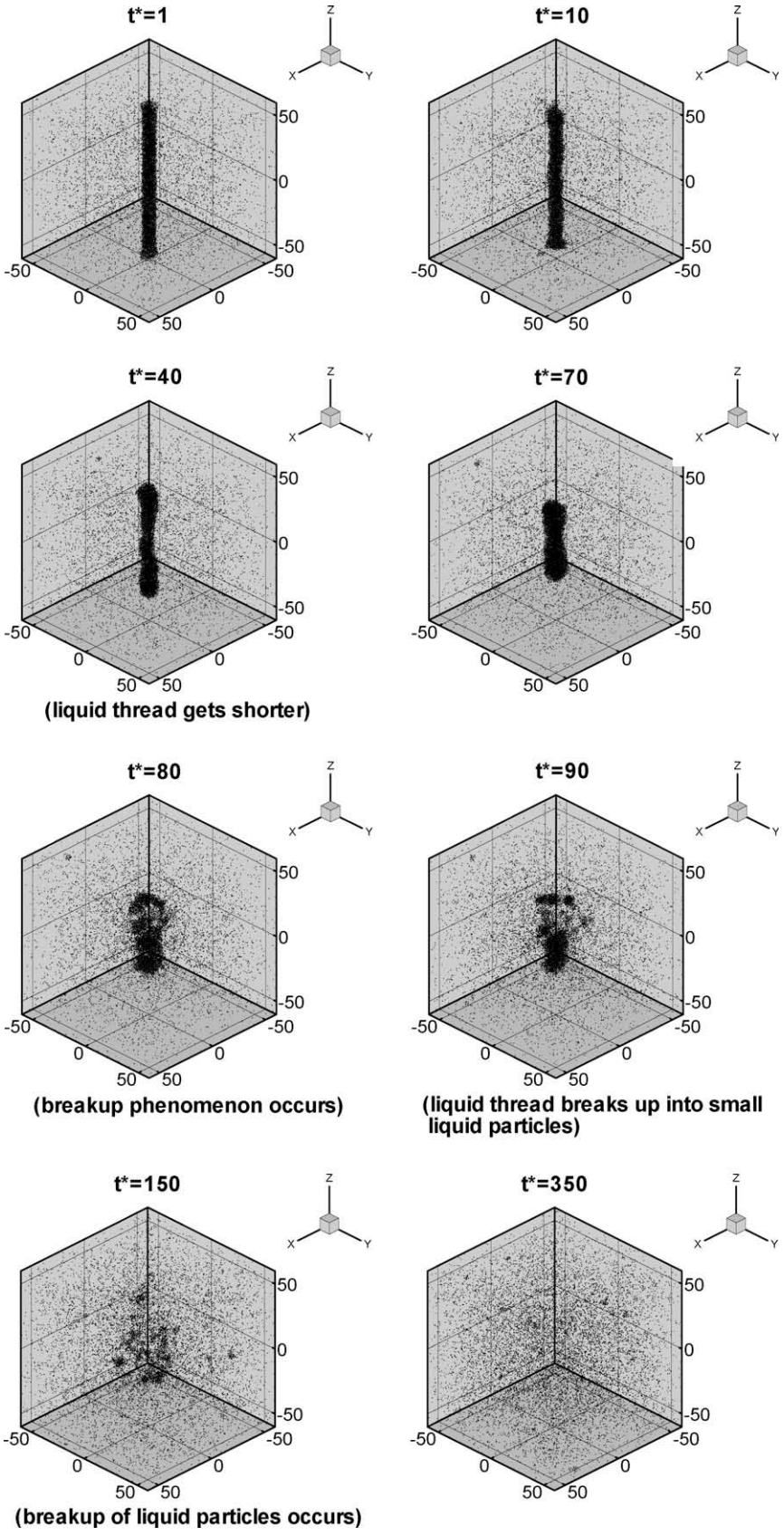

Fig. 5. Vaporization process for case 4 in Table 1.

indicated by the dashed circles for $100 \leqq t^* \leqq 140$ in Fig. 4. Breakup of the liquid particles occurs again at about $t^* = 150$. Collision, coalescence and breakup of the liquid particles play important roles in the vaporization process. Collision of liquid particles may lead to the formation of smaller liquid particles, which is conducive to vaporization. On the other hand, smaller liquid particles may also

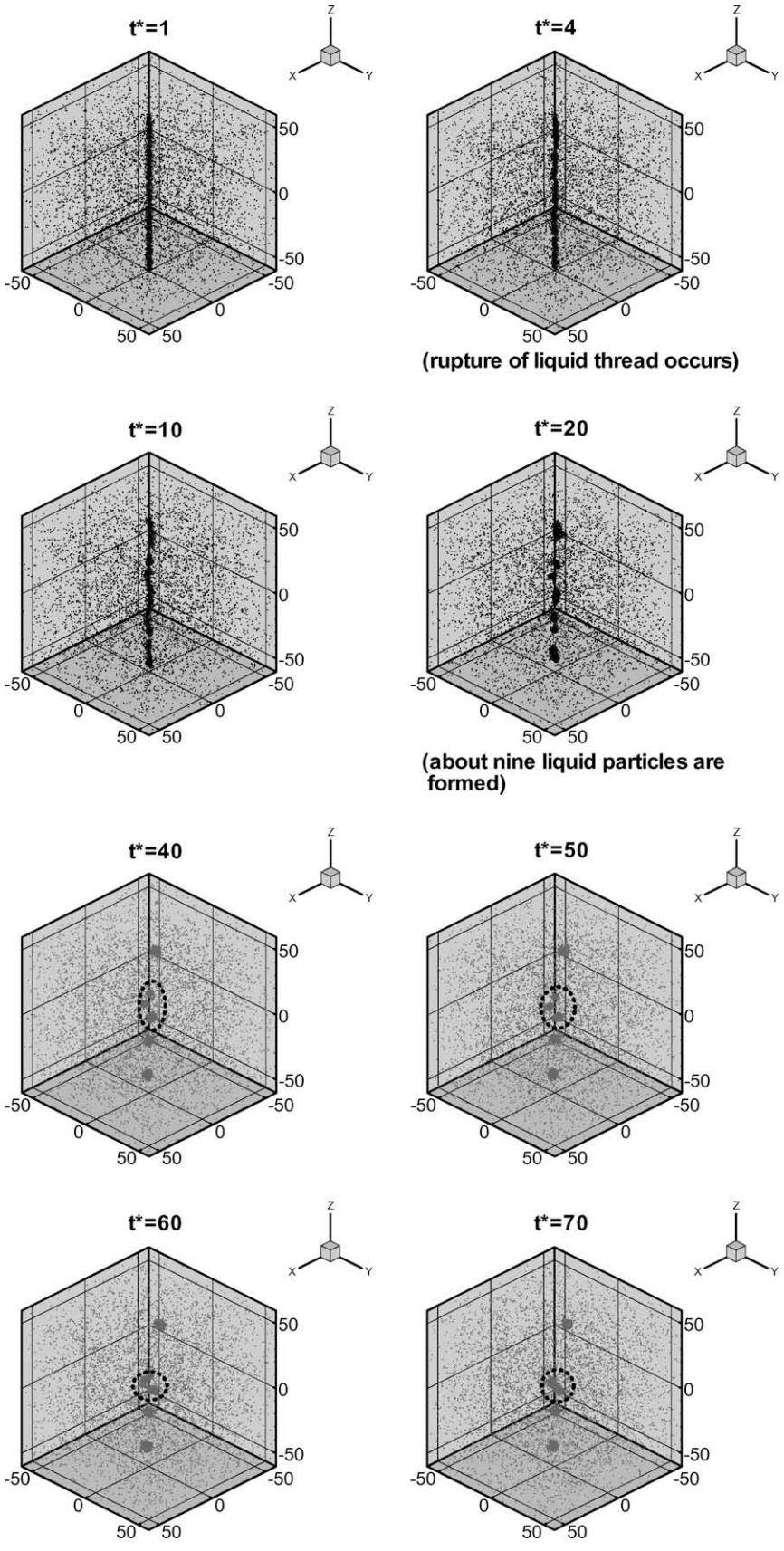

Fig. 6. Vaporization process for case 1 in Table 1.

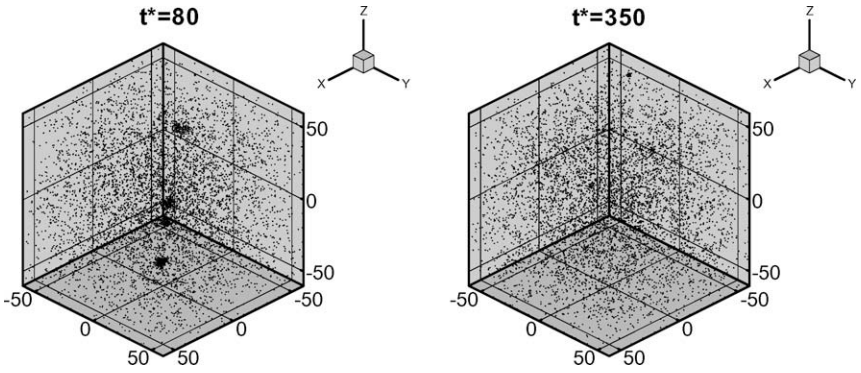

Fig. 6 (*continued*)

coalesce to larger liquid particles and then break up into even smaller liquid particles. This is also conducive to vaporization. The vaporization process for a liquid thread of $R^* = 5$, as shown in Fig. 5, is similar to that for $R^* = 4$.

From Fig. 3, we can observe that for a liquid thread of radius $R^* = 3$, the thread ruptures not only from the top and bottom surfaces of the fundamental cell but also from its middle section and they occur nearly simultaneously. On the other hand, for thicker liquid threads (Fig. 4 for $R^* = 4$ and Fig. 5 for $R^* = 5$), because the contraction velocity of the liquid thread in the axial direction is relatively large, rupture phenomenon does not occur in the interior of the fundamental cell and therefore only one dumbbell-shaped liquid particle is formed (see the snapshot at $t^* = 70$ in Figs. 4 and 5). This situation has been discussed in Kawano's work [8]: in the MD simulation using periodic boundary conditions, if the contraction velocity of the liquid thread in the axial direction is relatively large and the fundamental cell length is relatively small, there is a high possibility of the formation of only one liquid particle in the cell. Under such situation, the liquid thread will rupture from its two ends only, i.e. the top and bottom surfaces of the fundamental cell, but will not rupture from the interior of the fundamental cell. Koplik and Banavar's work [7] also revealed this observation.

If the radius of the liquid thread becomes smaller, say $R^* = 2$, rupture of the liquid thread occurs at about $t^* = 4$, which is earlier than for $R^* = 3$, as can be seen in Fig. 6. About nine liquid particles are formed at $t^* = 20$. It is also observed that collision, coalescence, and breakup of the liquid particles for $R^* = 2$ occur earlier than for larger liquid threads ($R^* = 3$, 4 and 5). Collision and coalescence of the liquid particles can be seen in the portions indicated by the dashed ellipses or circles for $40 \leqq t^* \leqq 70$ in Fig. 6. Breakup of the liquid particles occurs at about $t^* = 80$. Comparing Figs. 3–6, it can be seen that thicker liquid threads ($R^* = 4$ and 5) rupture from their ends only, i.e. the top and bottom surfaces of the fundamental cell; while thinner liquid threads ($R^* = 2$ and 3) rupture not only from their ends but also from the interior of the fundamental cell. In addition, it is observed that a thinner liquid thread evaporates faster. This will be further illustrated in later sections discussing the density distribution and the intermolecular force.

In some previous MD simulations of droplet vaporization [12–17], the droplet remains intact throughout the entire vaporization process. However, the simulation conditions in these papers are quite different from those in this research. As stated in Section 2, the procedure for MD simulation includes three stages: initialization, equilibration and production. In the above mentioned droplet vaporization researches, the droplet has been 'equilibrated' at the equilibration stage before it proceeds to the production stage, i.e. the droplet and its surrounding vapor are already in equilibrium at the beginning of the production stage. On the other hand, the droplets in this research are evolved from liquid thread. Therefore, the droplets and their surrounding vapor are not in equilibrium but rather are in motion at the beginning of the production stage. This implies larger intermolecular forces (surface tension) among molecules and larger interfacial forces between the droplets and their surrounding vapor. As pointed out by Lefebvre [18], Chigier [19,20] and Hiroyasu [21], surface tension and interfacial force are the major controlling mechanisms for breakup phenomenon. In addition, in the above mentioned droplet vaporization researches, only one droplet is simulated. On the other hand, two or more droplets are evolved from liquid thread in the present research. This provides more chances of collision, coalescence, and breakup of the droplets. Lefebvre [18] further pointed out that a cylindrical liquid body under amplified oscillations or perturbations may disintegrate into drops. This process is referred to as *primary* atomization. If the drops so formed exceed a critical size, they further disintegrate into drops of smaller size, a process known as *secondary* atomization [18]. From this research, it is found that both primary and secondary atomization occur for thicker liquid threads (see the snapshots at $t^* = 90$ and 150 in Figs. 4 and 5); while for thinner liquid threads ($R^* = 2$ and 3), only primary atomization occurs.

3.1.2. Liquid thread in vacuum

To investigate the influence of the surrounding medium on the vaporization process of a liquid thread, the preceding discussion is repeated by replacing the surrounding vapor molecules with vacuum. Fig. 7 shows the vaporization process of a liquid thread of $L^* = 120$ and $R^* = 3$ in vacuum. It is observed that the liquid thread does not rupture in the interior of the fundamental cell. The thread ruptures from their ends only, i.e. the top and bottom surfaces of the fundamental cell. This is contrary to the corresponding case of a liquid thread in vapor. This is because the contraction motion in the radial direction of the liquid thread is slower than that in its axial direction. Only one liquid particle is formed at about $t^* = 140$. At about $t^* = 290$, the liquid particle breaks up into smaller liquid particles and evaporates into the surroundings. Compared with the corresponding case of a liquid thread in vapor, a liquid thread in vacuum requires longer time to evaporate. This will be further illustrated in a later section discussing the density distribution. If the radius of the liquid thread becomes larger, say $R^* = 4$, again the thread ruptures from their ends only and not in the interior of the fundamental cell, as can be seen from Fig. 8. One liquid particle is formed at about $t^* = 140$ by the contraction motion of molecules in the axial direction of the liquid thread. Breakup phenomenon (primary atomization) occurs at about $t^* = 220$ and secondary atomization occurs at about $t^* = 290$. The vaporization process for a liquid thread of $R^* = 5$ is shown in Fig. 9. Similarly, only one liquid particle is formed at about $t^* = 190$. Breakup phenomenon occurs at about $t^* = 360$. The liquid particle disintegrates

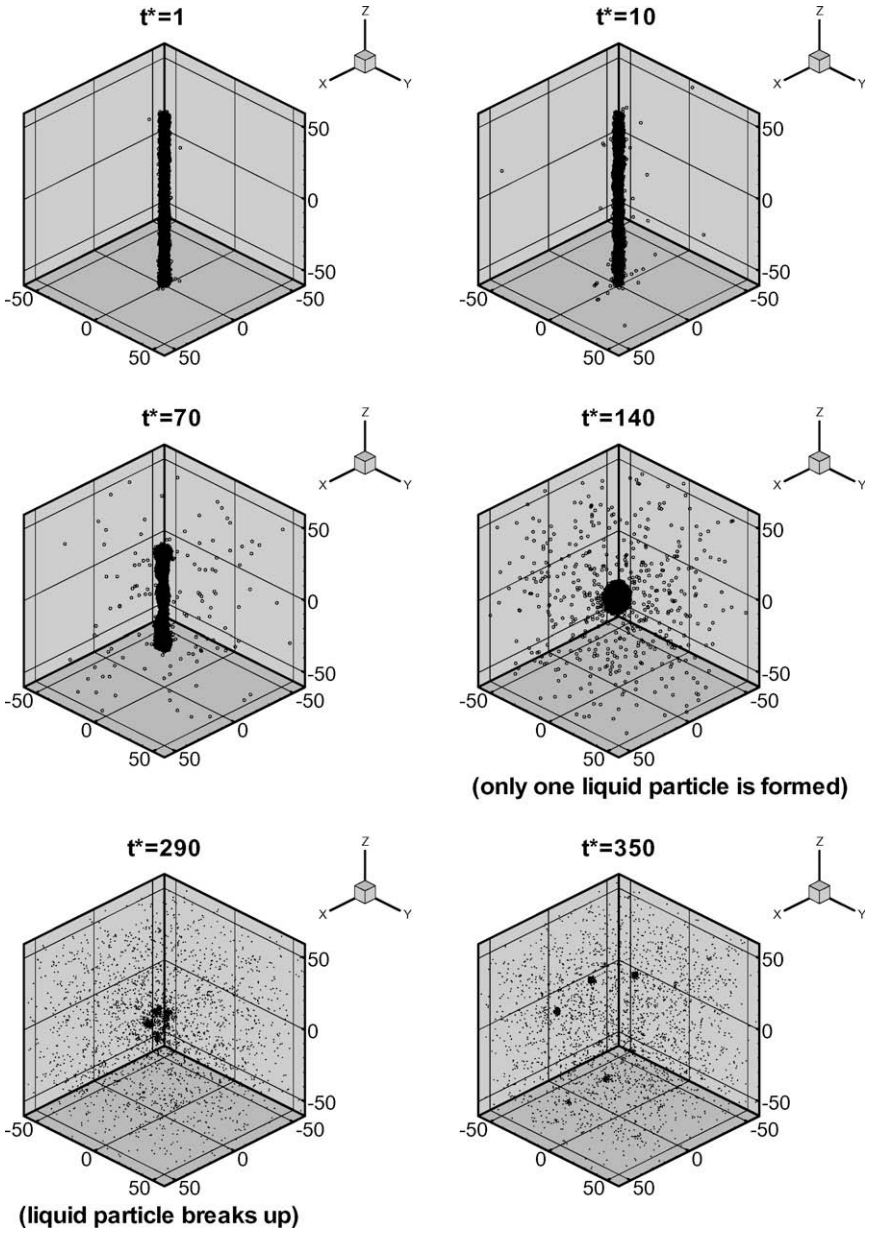

Fig. 7. Vaporization process for case 6 in Table 1.

into smaller liquid particles first and then evaporates into the surroundings (see $t^* = 380$ in Fig. 9). If the radius of the liquid thread becomes smaller, say $R^* = 2$, rupture of the liquid thread occurs at about $t^* = 10$, which is later than for the corresponding case in vapor. Seven liquid particles are formed at about $t^* = 20$, as can be seen in Fig. 10. These liquid particles eventually coalesce into five liquid particles and persist a long time before they evaporate completely.

Comparing the cases of different liquid thread radii, it is found that only primary atomization occurs for thinner liquid threads; while for thicker liquid threads, both primary and secondary atomization occur. Furthermore, it is observed that secondary atomization is less pronounced for liquid threads in vacuum because of the smaller intermolecular forces (surface tension) among molecules and the smaller interfacial forces between the droplets and their surrounding vapor, as compared to the case of liquid threads in vapor. In addition, comparison of a liquid thread in vacuum and a corresponding liquid thread in vapor shows that the latter evaporates faster. Molecular interactions play important roles in the vaporization process. When the remaining space is filled with vapor molecules, the surrounding vapor molecules provide more molecular interactions. This results in the formation of more liquid particles for a liquid thread in vapor. On the other hand, when the remaining space is a vacuum, less molecular interactions are provided and vaporization of the liquid thread in earlier stage of the vaporization process is mainly attributed to the molecular diffusion. Furthermore, an interesting phenomenon can be observed. When the remaining space is filled with vapor molecules, a thinner liquid thread evaporates faster, as discussed previously. However, when the liquid thread is in vacuum, a thinner liquid thread does not necessarily evaporate faster. For example, comparing the cases of $R^* = 3$ and 4, the case of $R^* = 4$ evaporates faster than that of $R^* = 3$, which is thinner. As stated above, the surrounding medium provides more molecular interactions and this is conducive to vaporization. When the remaining space is in vacuum, no surrounding vapor molecules exist initially and the surrounding med-

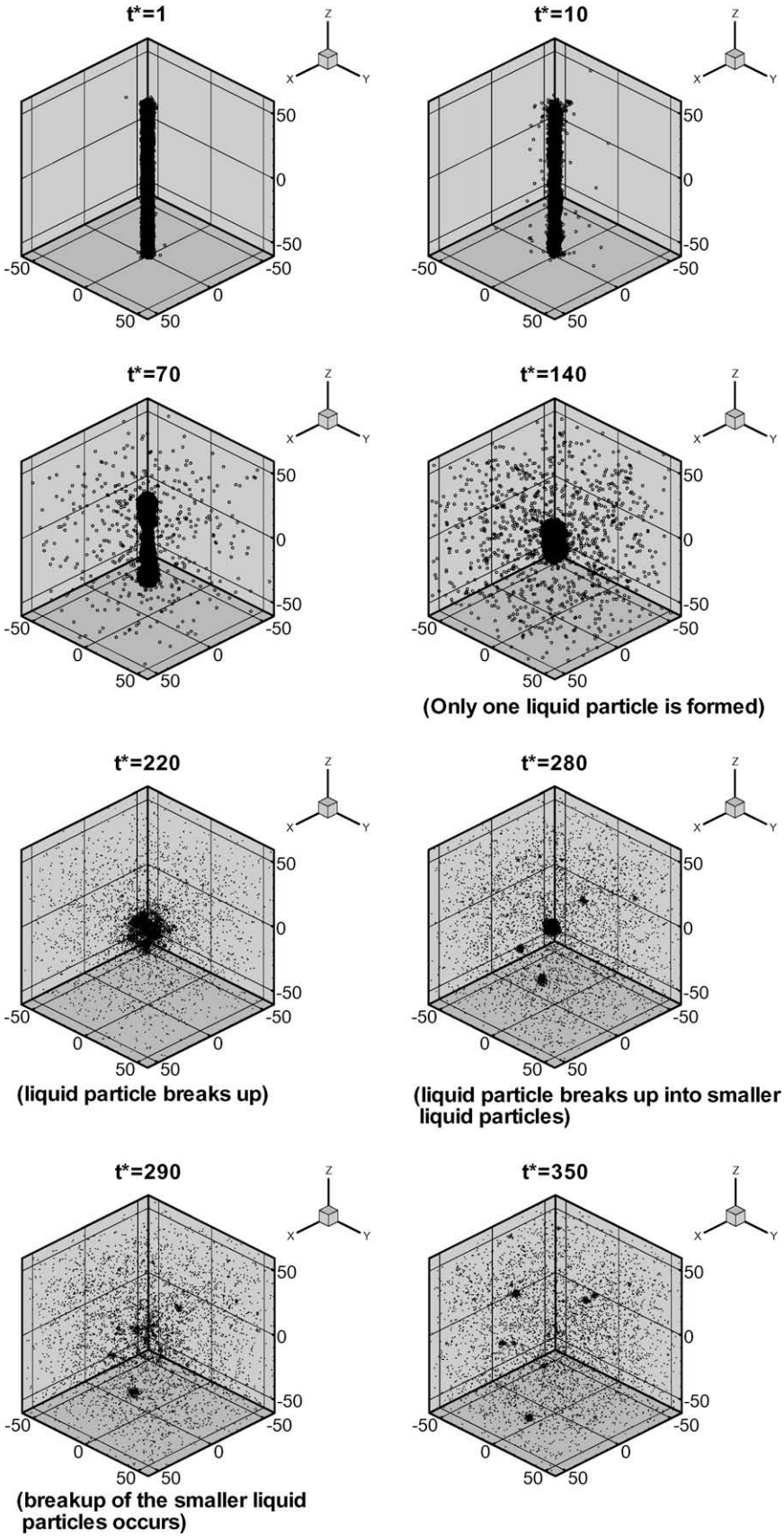

Fig. 8. Vaporization process for case 7 in Table 1.

ium comes entirely from the vaporization of the liquid thread. A thicker liquid thread may create more evaporated molecules to act as the role of the surrounding medium and this in turn provides more molecular interactions, which is conducive to vaporization.

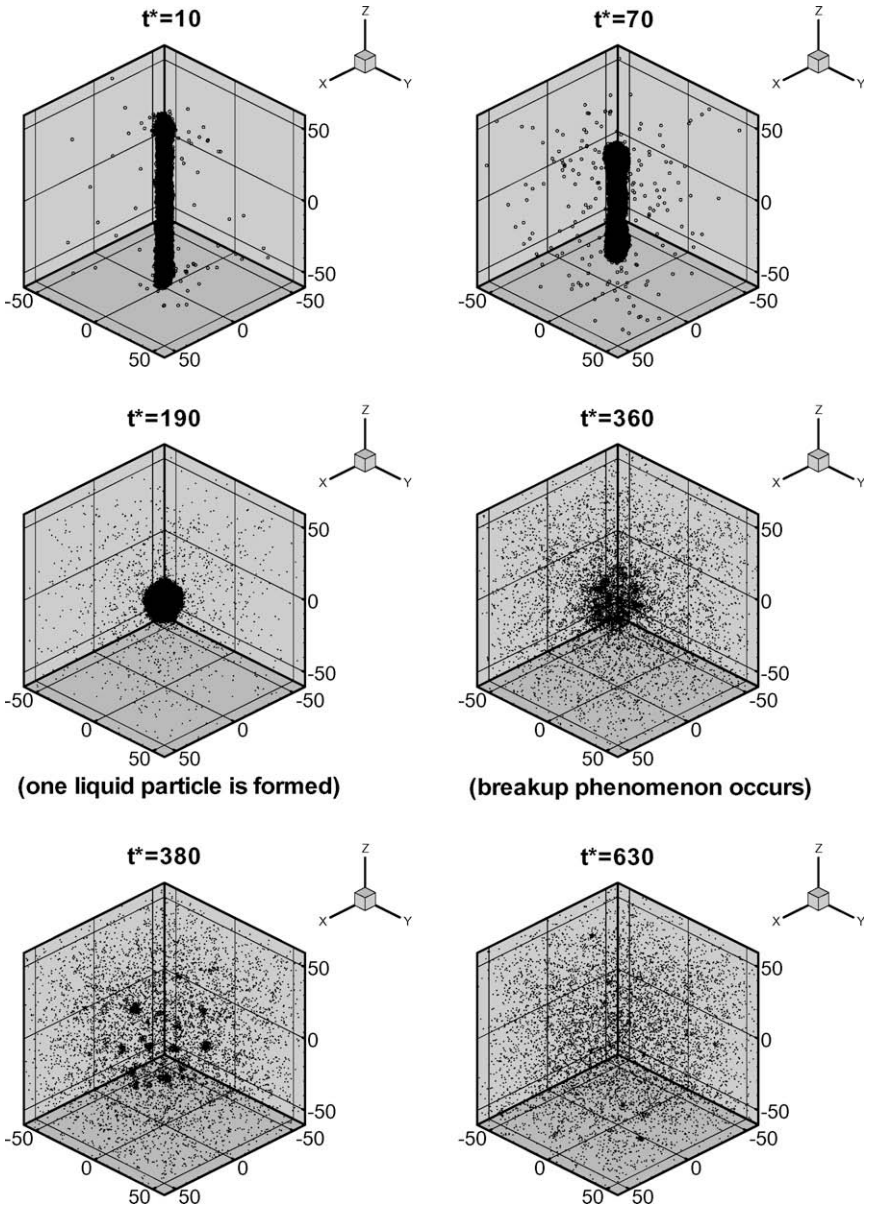

Fig. 9. Vaporization process for case 8 in Table 1.

The above discussion will be further illustrated in the following sections discussing the density distribution and the intermolecular force.

3.2. Density distribution

It is important that the system be in equilibrium state before statistical values of the local properties can be taken. However, owing to the computational capacity limitations, the MD simulation cannot proceed to a macroscopically long period. Nevertheless, the purpose of this paper is not to discuss statistical values of the local properties but to investigate the vaporization process of a liquid thread, which is one of the most fundamental and important phenomena during the atomization process. Criteria have to be made to quantify the discussion regarding the vaporization process of a liquid thread. Unfortunately, such criteria are still arbitrary in the literature. Because the system temperature in this study is kept at the desired temperature, a constant temperature criterion is not suitable for the discussion of the vaporization process. In this research, a liquid thread is considered to vaporize faster if the distribution of molecules reaches a uniform state quicker during the vaporization process. This criterion essentially concerns with the evolution of the density distribution. The density at a specified point in the fundamental cell can be defined as

$$\rho = \lim_{\delta V \to 0} \frac{\delta N}{\delta V} \tag{3}$$

where δV is a small volume surrounding the point considered and δN is the number of molecules inside the volume δV. The density defined by Eq. (3) is actually an averaged density of a small volume surrounding the point considered. The value will approach the density of a specified point if the volume δV shrinks to that point. However, for a meaningful density field, the volume δV cannot be too small because when δV becomes too small, it is difficult to obtain a definite value for $\delta N/\delta V$. In this study, the volume δV is taken to be a sphere with non-dimensionalized radius $R^* = 2$ and with its

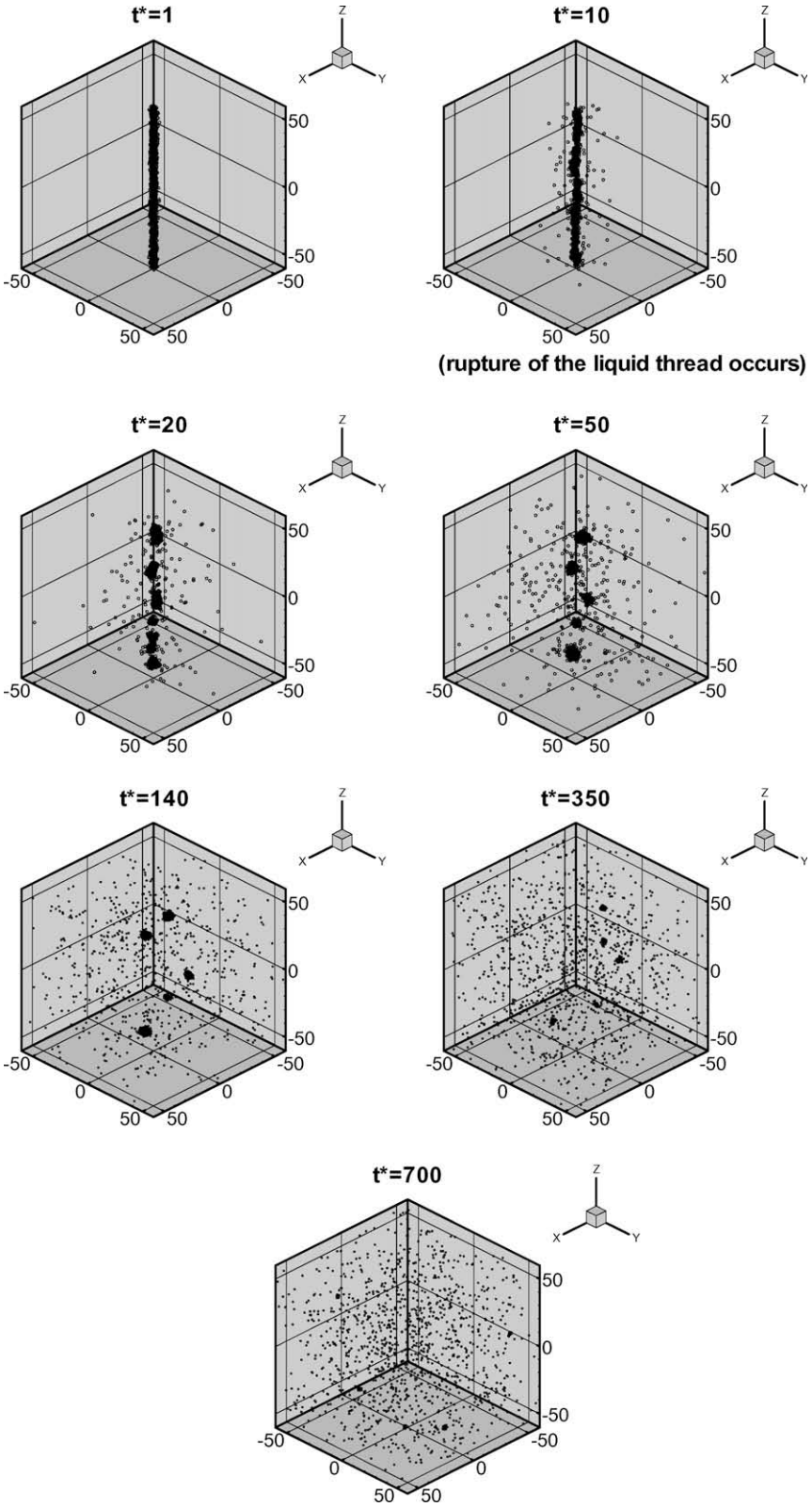

Fig. 10. Vaporization process for case 5 in Table 1.

center located at the point considered. This is an optimal choice after numerical test.

Fig. 11 shows the evolution of density uniformity factor for liquid threads with different radii and the conditions of $L^* = 120$, $\rho_L^* = 0.819$ and $\rho_V^* = 0.0031$. The density uniformity factor is defined as

$$f_\rho = \frac{\sum_N (\rho^* - \rho_{eq}^*)_{t^*} \Delta V}{\sum_N (\rho^* - \rho_{eq}^*)_{t^*=0} \Delta V} \tag{4}$$

where N is the total number of molecules in the fundamental cell, i.e. N_{mol} in Table 1, ρ^* and ΔV are the density and volume of molecule i, respectively, as defined by Eq. (3), and ρ_{eq}^* is the density value

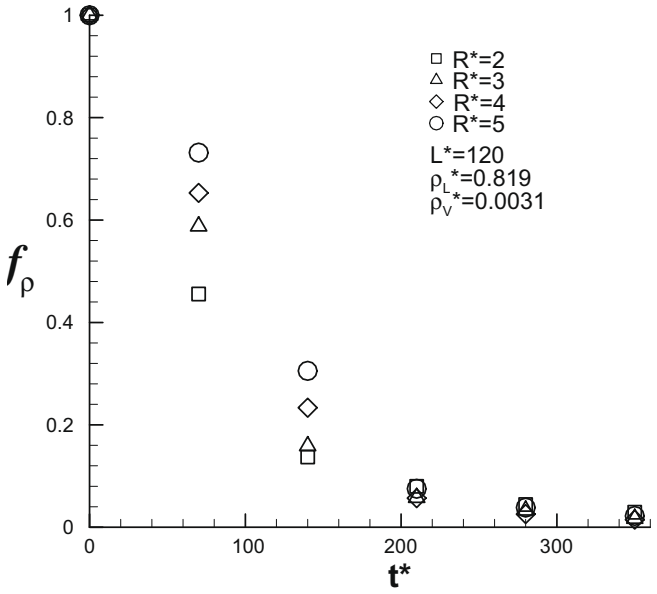

Fig. 11. Evolution of the density uniformity factor for case 1 to case 4 in Table 1.

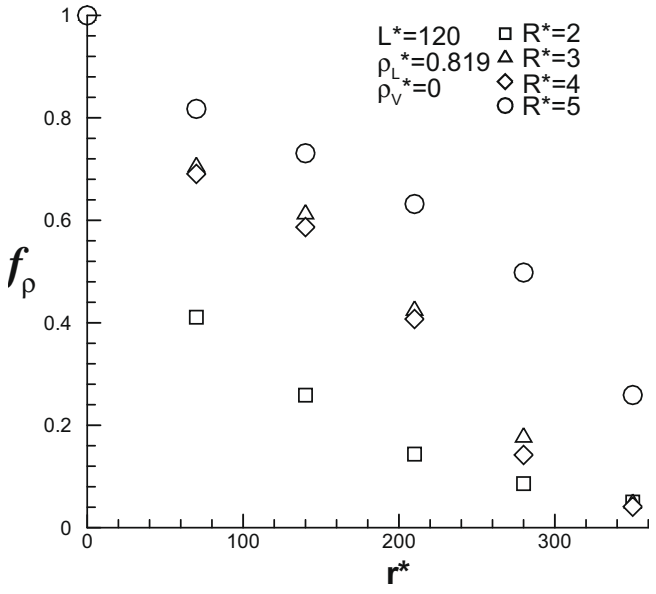

Fig. 12. Evolution of the density uniformity factor for case 5 to case 8 in Table 1.

when the molecules are uniformly distributed, i.e. $\rho^*_{eq} \equiv N_{\mathrm{mol/Vol}}$, where Vol is the volume of the fundamental cell. The density uniformity factor f_ρ as defined by Eq. (4) represents the deviation from uniform state. From Fig. 11 it is observed that a thinner liquid thread evaporates faster than a thicker one and this corroborates the results of Figs. 3–6 as discussed in Section 3.1.1. The time averaged value of the density uniformity factor, $\overline{f_\rho}$, in a time interval of $t^* = 0$–350, as listed in Table 1, also reveals this observation. Fig. 12 shows the situation for a liquid thread in vacuum. When the liquid thread is in vacuum, as discussed in Section 3.1.2, a thinner liquid thread does not necessarily evaporate faster. For example, compar-

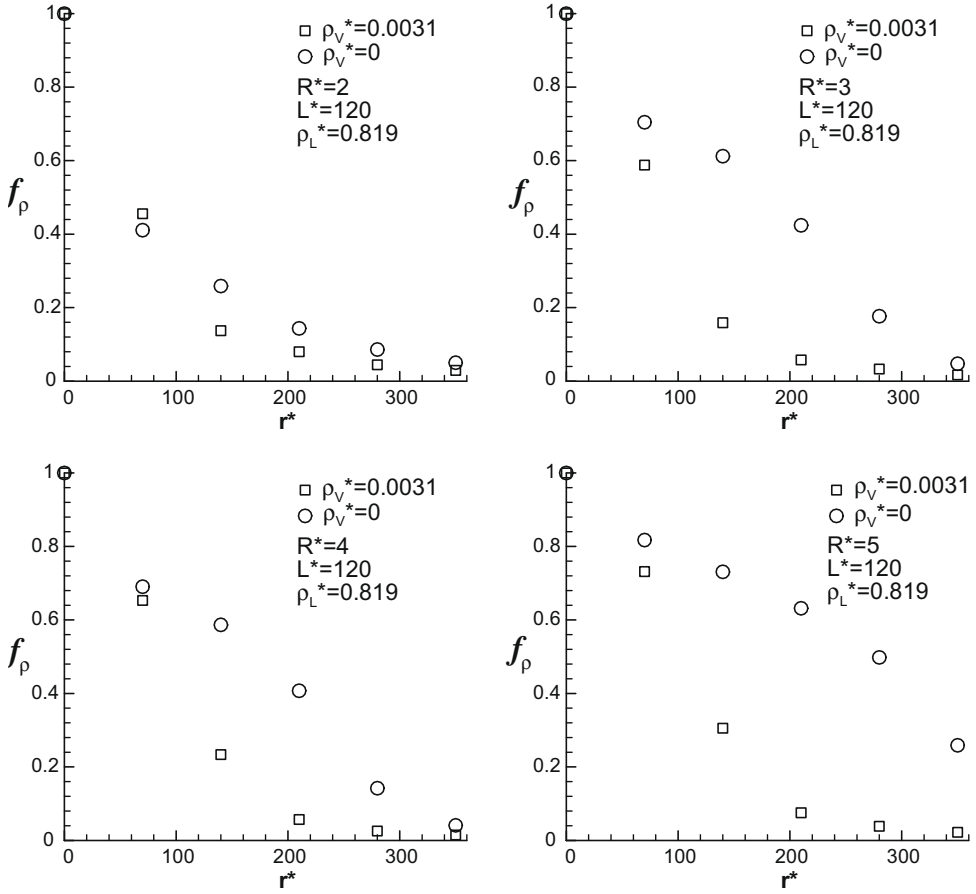

Fig. 13. Comparison of the evolution of density uniformity factor for a liquid thread in vapor and a liquid thread in vacuum.

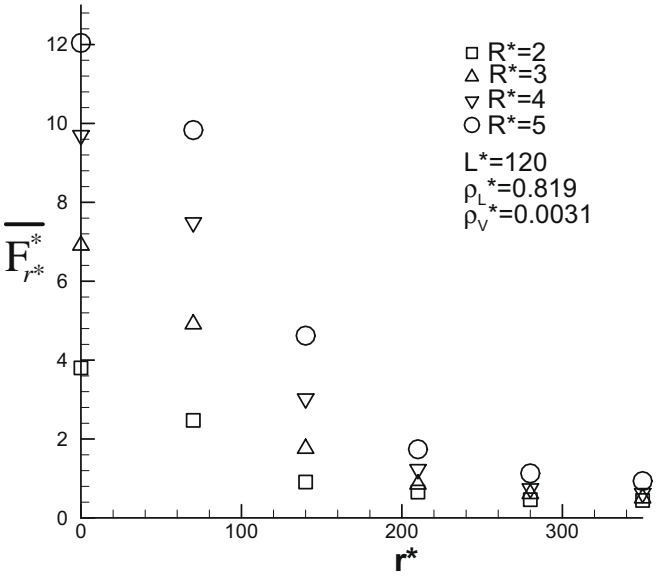

Fig. 14. Evolution of the averaged non-dimensionalized intermolecular force for case 1 to case 4 in Table 1.

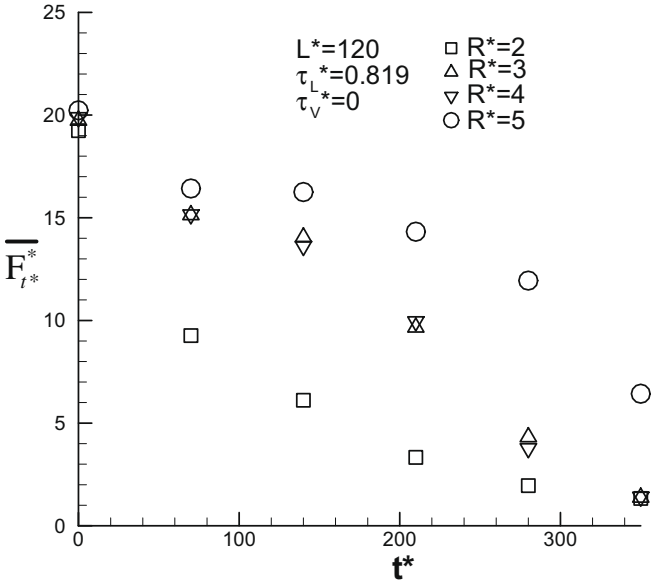

Fig. 15. Evolution of the averaged non-dimensionalized intermolecular force for case 5 to case 8 in Table 1.

ing the cases of $R^* = 3$ and 4, the case of $R^* = 4$ evaporates slightly faster than that of $R^* = 3$, which is thinner, as can be seen in Fig. 12. As mentioned earlier, the surrounding medium provides more molecular interactions and this is conducive to vaporization. When the remaining space is in vacuum, no surrounding vapor molecules exist initially and the surrounding medium comes entirely from the vaporization of the liquid thread. A thicker liquid thread may create more evaporated molecules to act as the role of the surrounding medium and this in turn provides more molecular interactions, which is conducive to vaporization.

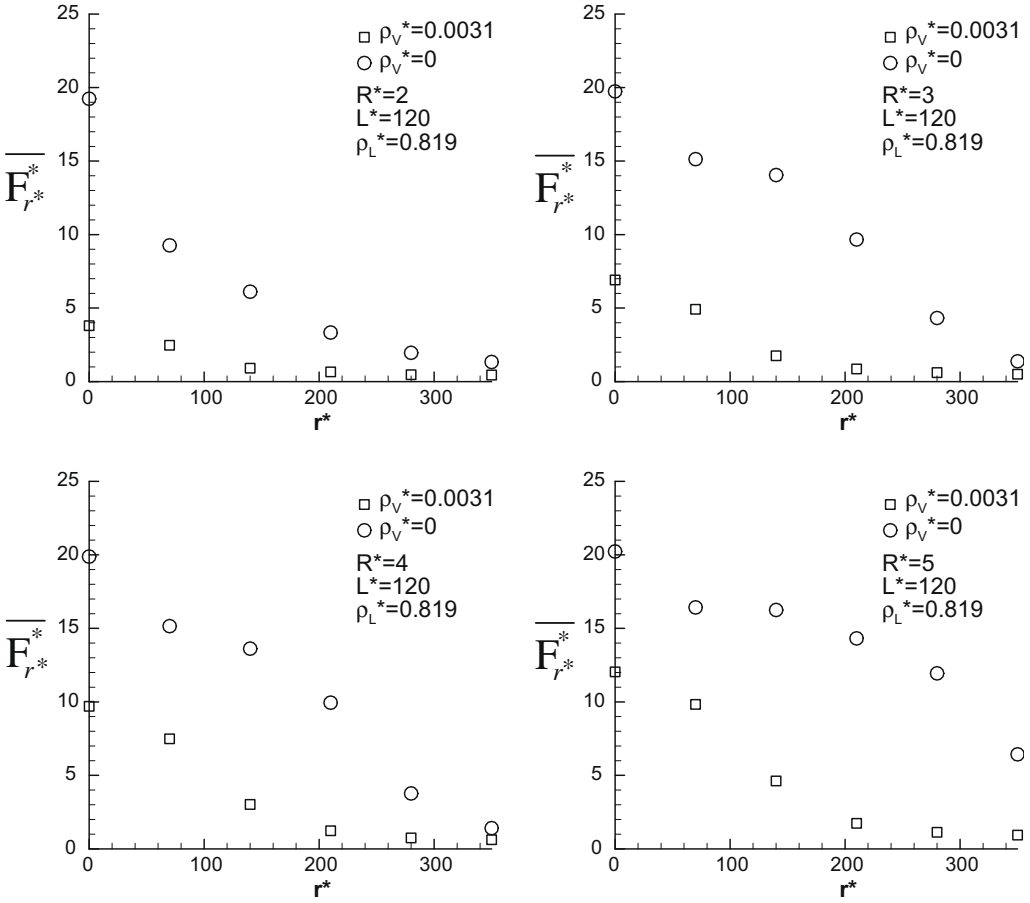

Fig. 16. Comparison of the evolution of averaged non-dimensionalized intermolecular force for a liquid thread in vapor and a liquid thread in vacuum.

To further investigate the influence of the surrounding medium on the vaporization process of a liquid thread, the comparison of the evolution of density uniformity factor for a liquid thread in vapor and a liquid thread in vacuum is shown in Fig. 13. It is observed that a liquid thread in vapor evaporates faster than a corresponding liquid thread in vacuum. This corroborates the conclusion made in Section 3.1.2, i.e. the surrounding medium provides more molecular interactions and this is conducive to vaporization. The time averaged value of the density uniformity factor, $\overline{f_\rho}$, as listed in Table 1, also reveals the above observation.

3.3. Intermolecular force

The intermolecular force is an indication of the surface tension experienced by the liquid particles and has a great effect upon the vaporization process [22]. Fig. 14 shows the evolution of averaged non-dimensionalized intermolecular force for liquid threads with different radii and the conditions of $L^* = 120$, $\rho^*_L = 0.819$ and $\rho^*_V = 0.0031$. The averaged non-dimensionalized intermolecular force at time t^* is defined as

$$\overline{F}^*_{t^*} = \frac{\sum_{i=1}^{N} F^*_{i,t^*}}{N} \tag{5}$$

where N is the total number of molecules in the fundamental cell and F^*_{i,t^*} is the resultant force of the non-dimensionalized intermolecular force vector acting on molecule i at time t^*, i.e. $F^*_{i,t^*} = (F^{*2}_{x,i,t^*} + F^{*2}_{y,i,t^*} + F^{*2}_{z,i,t^*})^{1/2}$, where $F^*_{x,i,t^*}, F^*_{y,i,t^*}$ and F^*_{z,i,t^*} are the components of the intermolecular force vector at the x, y and z directions, respectively, acting on molecule i at time t^*. The intermolecular force diminishes with time because of the increase of distances between molecules as the liquid thread vaporizes. From Fig. 14, it is observed that a thinner liquid thread evaporates faster than a thicker one and this corroborates the results of Figs. 3–6 as discussed in Section 3.1.1 and Fig. 11 in Section 3.2. The time averaged value of the averaged non-dimensionalized intermolecular force, $\overline{F^*}$, in a time interval of $t^* = 0$–350, as listed in Table 1, also reveals this observation. Fig. 15 shows the situation for a liquid thread in vacuum. When the liquid thread is in vacuum, as discussed in Sections 3.1.2 and 3.2, a thinner liquid thread does not necessarily evaporate faster. For example, comparing the cases of $R^* = 3$ and 4, the case of $R^* = 4$ evaporates slightly faster than that of $R^* = 3$, which is thinner, as can be seen in Fig. 15. This exception has been explained in detail in Sections 3.1.2 and 3.2.

To investigate the influence of the surrounding medium on the vaporization process of a liquid thread, the comparison of the evolution of averaged non-dimensionalized intermolecular force for a liquid thread in vapor and a liquid thread in vacuum is shown in Fig. 16. It is observed that a liquid thread in vapor evaporates faster than a corresponding liquid thread in vacuum and this corroborates the conclusion made in Sections 3.1.2 and 3.2, i.e. the surrounding medium provides more molecular interactions and this is conducive to vaporization. The time averaged value of the averaged non-dimensionalized intermolecular force, $\overline{F^*}$, as listed in Table 1, also reveals the above observation.

Another observation can be made from Figs. 14–16. In the discussion of vaporization process for a liquid thread in vapor in Section 3.1.1, it has been observed that rupture, breakup, collision, and coalescence phenomena occur in the earlier stage of the vaporization process. Correspondingly, the intermolecular force has a higher level in the earlier stage of the vaporization process, as can be seen in Fig. 14. After molecular interaction, the molecules become more evenly distributed and the intermolecular force diminishes. Obviously, there are close correspondence between the molecular interaction and the intermolecular force. In the earlier stage of vaporization process, the molecules are closer to each other and thus the intermolecular force has higher levels. In the same way, when the molecules are closer to each other, there are more molecular interactions. Furthermore, comparing the case of a liquid thread in vacuum with that of a liquid thread in vapor, it has been shown in previous sections that the former case evaporates slower. In Section 3.1.2, it has been observed that for a liquid thread in vacuum, rupture, breakup, collision, and coalescence phenomena occur later, as compared to the case of a liquid thread in vapor. This corresponds to a higher level of intermolecular force persisting a longer time, as can be seen from Figs. 15 and 16. The evolution of density uniformity factor for liquid threads in vacuum, as shown in Figs. 12 and 13, also reveals this tendency.

3.4. Stability analysis

The linear stability of a liquid jet was first studied by Rayleigh [23]. A liquid thread of Radius R is unstable and will break up into drops to minimize the surface energy if the axial wavelength of the surface perturbation $L \geqq 2\pi R$. If $L < 2\pi R$, the thread is stable and will remain intact. Before breakup, liquid is collected into large bulbs that are connected by thin liquid filaments. The filaments pinch off at the two ends to form satellite droplets [9]. Owing to the periodic boundary conditions in this study, the fundamental cell size L^* can be regarded as the longest wavelength of the perturbation. Because $L^* \geqq 2\pi R^*$ for all the cases studied in this research, the liquid threads are all unstable and ultimately break up, as discussed in previous sections. This agrees with Rayleigh's stability criterion of liquid threads.

4. Conclusions

In this study, the vaporization process of a liquid thread is investigated by MD simulation with periodic boundary conditions applied in all three directions. The present analysis focuses not only on the liquid particle formation but also on its subsequent evolution, which involves breakup, collision, and coalescence of the liquid particles. These phenomena play important roles in the entire vaporization process. The present study provides a detailed illustration for the vaporization process of a liquid thread and is helpful to the understanding of the liquid atomization process. It is found that a thicker liquid thread ruptures from its two ends only, i.e. the top and bottom surfaces of the fundamental cell; while a thinner liquid thread ruptures not only from its two ends but also from the interior of the fundamental cell. Both primary and secondary atomization occur for thicker liquid threads; while for thinner liquid threads, only primary atomization occurs. Secondary atomization is less pronounced for liquid threads in vacuum. A liquid thread in vapor ruptures earlier and produces more liquid particles than a corresponding liquid thread in vacuum. In addition, a liquid thread in vapor evaporates faster than a corresponding liquid thread in vacuum. A thinner liquid thread in vapor evaporates faster than a thicker one; while a thinner liquid thread in vacuum does not necessarily evaporate faster than a thicker one. Finally, the result of this research reveals that Rayleigh's stability criterion holds down to the molecular scale.

Acknowledgement

The author gratefully acknowledges the grant support from the National Science Council, Taiwan, ROC, under the Contract NSC97-2221-E-150-029.

References

[1] C.L. Yeh, Turbulent flow simulation of liquid jet emanating from pressure-swirl atomizer, Heat Mass Transfer 44 (3) (2008) 275–280.

[2] C.L. Yeh, Numerical simulation of turbulent liquid jet emanating from plain-orifice atomizer and pressure-swirl atomizer, Numer. Heat Transfer A 51 (2007) 1187–1212.
[3] C.L. Yeh, Turbulent flow investigation inside and outside plain-orifice atomizers with rounded orifice inlets, Heat Mass Transfer 41 (9) (2005) 810–823.
[4] C.L. Yeh, Numerical investigation of liquid jet emanating from plain-orifice atomizers with chamfered or rounded orifice inlets, JSME Int. J. B 47 (1) (2004) 37–47.
[5] C.L. Yeh, Effect of inlet turbulence intensity on discharge coefficients for liquid jet emanating from a plain-orifice atomizer: a numerical study, J. Aeronaut. Astronaut. Aviat. 35 (3) (2003) 299–306.
[6] C.L. Yeh, Numerical study of inlet and geometry effects on discharge coefficients for liquid jet emanating from a plain-orifice atomizer, J. Mech. A 18 (3) (2002) 153–161.
[7] J. Koplik, J.R. Banavar, Molecular dynamics of interface rupture, Phys. Fluids A 5 (3) (1993) 521–536.
[8] S. Kawano, Molecular dynamics of rupture phenomena in a liquid thread, Phys. Rev. E 58 (4) (1998) 4468–4472.
[9] D. Min, H. Wong, Rayleigh's instability of Lennard–Jones liquid nanothreads simulated by molecular dynamics, Phys. Fluids 18 (2006) 024103.
[10] B.G. Kim, J.S. Lee, M. Han, S. Park, A molecular dynamics study on stability and thermophysical properties of nano-scale liquid threads, Nano-scale Micro-scale Thermophys. Eng. 10 (2006) 283–304.
[11] J.M. Haile, Molecular Dynamics Simulation, John Wiley & Sons, New York, 1992. chapter 5.
[12] S. Sumardino, J. Fischer, Molecular simulations of droplet evaporation processes: adiabatic pressure jump evaporation, Int. J. Heat Mass Transfer 49 (2006) 1148–1161.
[13] L.N. Long, M.M. Micci, B.C. Wong, Molecular dynamics simulations of droplet evaporation, Comput. Phys. Commun. 96 (1996) 167–172.
[14] E.S. Landry, S. Mikkilineni, M. Paharia, A.J.H. McGaughey, Droplet evaporation: a molecular dynamics investigation, J. Appl. Phys. 102 (2007) 124301.
[15] J.H. Walther, P. Koumoutsakos, Molecular dynamics simulation of nanodroplet evaporation, J. Heat Transfer 123 (2001) 741–748.
[16] A.P. Bhasali, Y. Bayazitoglu, S. Maruyama, Molecular dynamics simulation of an evaporating sodium droplet, Int. J. Therm. Sci. 38 (1999) 66–74.
[17] L. Consolini, S.K. Aggarwal, S. Murad, A molecular dynamics simulation of droplet evaporation, Int. J. Heat Mass Transfer 46 (2003) 3179–3188.
[18] A.H. Lefebvre, Atomization and Sprays, Hemisphere, New York, 1989. chapter 2.
[19] N. Chigier, Breakup of liquid sheets and jet, AIAA Paper 99-3640, 1999.
[20] F. Ruiz, N. Chigier, Parametric experiments on liquid jet atomization spray angle, Atomization Sprays 1 (1991) 23–45.
[21] H. Hiroyasu, Spray breakup mechanism from the hole-type nozzle and its applications, Atomization Sprays 10 (2000) 511–527.
[22] M.M. Micci, T.L. Kaltz, L.N. Long, Molecular dynamics simulations of atomization and spray phenomena, Atomization Sprays 11 (2001) 351–363.
[23] Lord Rayleigh, On the stability of jets, Proceedings of the London Mathematical Society 10 (1879) 4–13.